

# Correlation in formation of ${}^8\text{Be}$ nuclei and $\alpha$ -particles in fragmentation of relativistic nuclei

A.A. Zaitsev,<sup>1,2</sup> D.A. Artemenkov,<sup>1</sup> V.V. Glagolev,<sup>1</sup> M.M. Chernyavsky,<sup>2</sup>  
N.G. Peresadko,<sup>2</sup> V.V. Rusakova,<sup>1</sup> and P.I. Zarubin<sup>1,2,\*</sup>

<sup>1</sup>*Joint Institute for Nuclear Research, Dubna, Russia*

<sup>2</sup>*Lebedev Physical Institute, Russian Academy of Sciences, Moscow, Russia*

(Dated: February 19, 2021)

## Abstract

In the events of peripheral dissociation of relativistic nuclei in the nuclear track emulsion, it is possible to study the emerging ensembles of He and H nuclei, including those from decays of the unstable  ${}^8\text{Be}$  and  ${}^9\text{B}$  nuclei, as well as the Hoyle state. These extremely short-lived states are identified by invariant masses calculated from the opening angles in  $2\alpha$ -pairs,  $2\alpha p$ - and  $3\alpha$ -triplets in the approximation of conservation of momentum per nucleon of the primary nucleus. In the same approach, it is possible to search for more complex states. This paper explores the correlation between the formation of  ${}^8\text{Be}$  nuclei and the multiplicity of accompanying  $\alpha$ -particles in the dissociation of relativistic  ${}^{16}\text{O}$ ,  ${}^{22}\text{Ne}$ ,  ${}^{28}\text{Si}$ , and  ${}^{197}\text{Au}$  nuclei. On this basis, estimates of such a correlation are presented for the unstable  ${}^9\text{B}$  nucleus and the Hoyle state. An enhancement in the  ${}^8\text{Be}$  contribution to dissociation with the  $\alpha$ -particle multiplicity is found. Decays of  ${}^9\text{B}$  nuclei and Hoyle states follow the same trend.

PACS numbers: 21.60.Gx, 25.75.-q, 29.40.Rg

---

\* email: zarubin@lhe.jinr.ru

## I. INTRODUCTION

The analysis of fragmentation of relativistic nuclei in a nuclear track emulsion (NTE) makes it possible to study internally non-relativistic ensembles of H and He nuclei starting with produced in decays of the unstable  ${}^8\text{Be}$  and  ${}^9\text{B}$  nuclei and up to the most complex ones [1–3]. NTE layers with a thickness of 200 to 500  $\mu\text{m}$ , longitudinally exposed to the nuclei under study, make it possible to determine with full completeness and resolution of 0.5  $\mu\text{m}$  the angles between the directions of emission of relativistic fragments in the cone  $\sin\theta_{fr} = P_{fr}/P_0$ , where  $P_{fr} = 0.2 \text{ GeV}/c$  is the characteristic Fermi momentum of nucleons in a projectile nucleus with a momentum per nucleon. The most valuable in this aspect are the events of dissociation which are not accompanied by fragments of the target nuclei and generated mesons. They are called coherent dissociation or “white” stars.

Despite the fact that coherent dissociation  ${}^{12}\text{C} \rightarrow 3\alpha$  and  ${}^{16}\text{O} \rightarrow 4\alpha$  is only 1–2% of inelastic interactions, a targeted search performed by transverse scanning made it possible to investigate by the invariant mass method 310  $3\alpha$  and 641  $4\alpha$  “white” stars [4, 5] and establish in both cases the contributions of  $3\alpha$ -decays of the Hoyle state (HS) [6, 7]. In general, the invariant mass  $Q = M^* - M$  is given by the sum  $M^{*2} = \Sigma(P_i \cdot P_k)$ , where  $P_{i,k}$  are 4-momenta of fragments, and  $M$  is their mass. To calculate the invariant masses of  $2\alpha$ -pairs  $Q_{2\alpha}$  and  $3\alpha$ -triplets  $Q_{3\alpha}$  in the approximation of conservation of momentum per nucleon by  $\alpha$ -particles of the primary nucleus, only measurements of their emission angles are used. The correspondence between He -  ${}^4\text{He}$  and H -  ${}^1\text{H}$  is assumed, since in the case of extremely narrow decays of  ${}^8\text{Be}$  and  ${}^9\text{B}$ , the measured contributions of  ${}^3\text{He}$  and  ${}^2\text{H}$  are small. The initial portions of the event distributions over the variables  $Q_{2\alpha}$  and  $Q_{3\alpha}$  contain peaks corresponding to  ${}^8\text{Be}$  and HS for both  ${}^{12}\text{C}$  and  ${}^{16}\text{O}$ . Since the decay energy values are noticeably lower than the nearest excitations, the selection  $Q_{2\alpha}({}^8\text{Be}) \leq 0.2 \text{ MeV}$  and  $Q_{3\alpha}(\text{HS}) \leq 0.7 \text{ MeV}$  is possible. Their application gives a contribution of  ${}^8\text{Be}$  (HS)  $45 \pm 4\%$  ( $11 \pm 3\%$ ) for  ${}^{12}\text{C}$  and  $62 \pm 3\%$  ( $22 \pm 2\%$ ) for  ${}^{16}\text{O}$ .

The invariant representation makes it possible to identify among the relativistic fragments the decays  ${}^8\text{Be}$ ,  ${}^9\text{B}$ , and HS, including cascade ones, regardless of the initial collision energy. It becomes possible to establish a connection with the low energy studies [9–11]. The effect of relativistic collimation makes it possible not only to study the generation of  ${}^8\text{Be}$ ,  ${}^9\text{B}$  and HS, but also to search for unstable states of increasing complexity decaying through them

[12–14].

Earlier, the contribution of  ${}^8\text{Be}$  and  ${}^9\text{B}$  decays to the dissociation of few light, middle (Ne, Si) and heavy (Au) nuclei were estimated in a similar way (review [8]). Each of these extremely unstable states has low decay energy and lifetime (inversely proportional to the decay width) is several orders higher than the characteristic time of generating reactions. They are predicted to be unusually large in size (example in [12]). One can assume the presence of these unstable states as virtual components in parent nuclei, which manifest themselves in relativistic fragmentation. However, maintaining such universality with an increase in the mass number of nuclei under study seems to be more and more problematic.

An alternative consists in the  ${}^8\text{Be}$  formation during the final state interaction of the produced  $\alpha$ -particles and the subsequent pick-up of accompanying  $\alpha$ -particles and nucleons with the emission of the necessary  $\gamma$ -quanta. The consequence of such a scenario would be an increase in the  ${}^8\text{Be}$  yield with a multiplicity of  $\alpha$ -particles  $n_\alpha$  in the event, and possibly  ${}^9\text{B}$  and HS decaying through  ${}^8\text{Be}$ . The purpose of this study is to identify a possible relationship between the formation of the unstable sates and accompanying multiplicity.

The smaller the difference between the charges and mass numbers of the parent nucleus and the reconstructed unstable state, the easier they are identified (for example,  ${}^9\text{Be} \rightarrow {}^8\text{Be}$  and  ${}^{10}\text{C} \rightarrow {}^9\text{B}$  [8]), since the distortions in determining the fragment emission angles, which tend to increase in the transition from track to track, are minimized. In addition, in the studied region of invariant masses, the combinatorial background from the accompanying multiplicity is minimized. However, this limitation is holding back testing the universality and correlations in the unstable state production and the search for more complex states of this kind. NTE layers exposed to heavy nuclei make it possible to radically expand the multiplicity of the studied fragments, which demands to study in practice identification conditions with increasing  $n_\alpha$ .

A primary track scanning in NTE allows one to find interactions without sampling, in particular, with a different number of relativistic fragments of He and H. The data obtained in this approach allow tracing the contribution of the unstable states and provide support in advancing to greater statistics and more complex states by the transverse scanning method. Although the multiple channel statistics of turns out to be radically lower but its evolution can be followed. Further, overview measurements gathered by the emulsion collaboration at the JINR Synchrophasotron in the 80s and EMU collaboration at the AGS (BNL) and

SPS (CERN) synchrotrons in the 90s on the fragmentation of relativistic nuclei  $^{16}\text{O}$ ,  $^{22}\text{Ne}$ ,  $^{28}\text{Si}$  and  $^{197}\text{Au}$  are mainly used [15–19]. Photos and videos of characteristic interactions are available [1, 20].

Large-scale and uniform, this data retains its uniqueness in terms of relativistic nuclear fragmentation. Among the many results obtained the conclusion about the limiting fragmentation regime in the widest possible range of nuclei and primary energy values, which is expressed by the invariability of the charge composition of fragments and the scale-invariant behavior of their spectra, remains of fundamental value. At the same time, despite the diversity of the results obtained, fine effects associated with angular correlations within the ensembles of fragments remained unexplored. In addition to the actual interest in the topic, they require a targeted build-up of statistics in multiple channels. Owing to the use of NTE layers exposed at that time, the statistics of the measured interactions  $^{28}\text{Si} \rightarrow n_\alpha$  ( $\geq 3$ ) is started to be supplemented in the framework of our BECQUEREL experiment at JINR. All these measurements, uniformly represented in the variable of invariant mass, make it possible to assess the role of unstable states in nuclear fragmentation and formulate the further study tasks.

## II. $^{16}\text{O}$ FRAGMENTATION

There are measurements for inelastic interactions at four energy values of  $^{16}\text{O}$  nuclei found when tracing primary tracks including 2823 at 3.65 GeV/nucleon (JINR Synchrophasotron, 80s), 689 at 14.6 GeV/nucleon (BNL AGS, 90s), 885 at 60 GeV/nucleon and 801 at 200 GeV/nucleon (CERN SPS). The distributions of all  $2\alpha$ -pair combinations from these interactions  $N_{(2\alpha)}$  over the invariant mass  $Q_{2\alpha} \leq 1$  MeV are stacked together in Fig. 1. As in the case of high statistics  $^{16}\text{O} \rightarrow 4\alpha$  [8], a peak is observed at the origin, and the condition  $Q_{2\alpha}(^8\text{Be}) \leq 0.2$  MeV is accepted for selecting  $^8\text{Be}$  decay candidates.

Table I shows the number of events  $N_{n\alpha}(^8\text{Be})$  containing at least one  $^8\text{Be}$  decay candidate satisfying the condition  $Q_{2\alpha}(^8\text{Be}) \leq 0.2$  MeV, among the events  $N_{n\alpha}$  with the relativistic  $\alpha$ -particle multiplicity  $n_\alpha$ . In the covered range of initial energy the distributions  $N_{n\alpha}$  and  $N_{n\alpha}(^8\text{Be})$  show similarities, which corresponds to the concept of the limiting nuclear fragmentation regime. As  $n_\alpha$  increases, the fraction of events with  $^8\text{Be}$  decays increases. The invariability of the composition of relativistic fragmentation from the initial energy

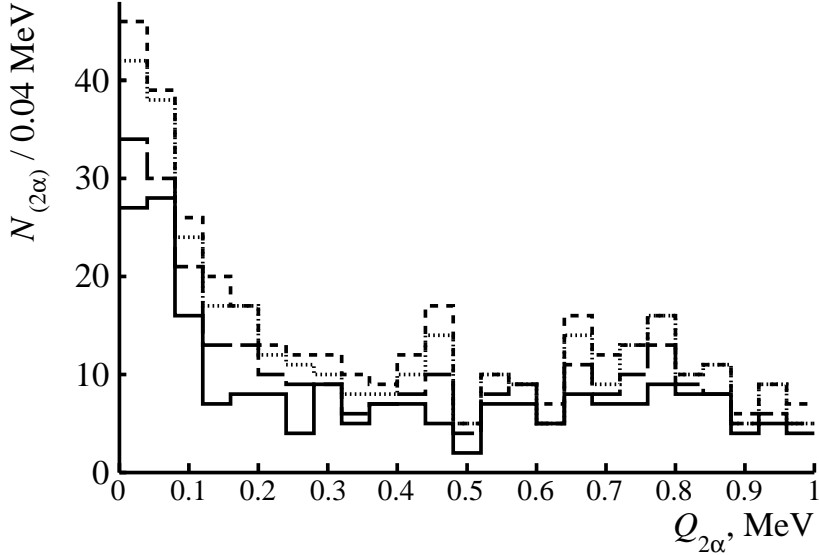


FIG. 1. Distribution of  $2\alpha$ -pairs  $N_{(2\alpha)}$  over invariant mass  $Q_{2\alpha}$  ( $\leq 1$  MeV) in fragmentation of 3.65 GeV/nucleon  $^{16}\text{O}$  nuclei (solid line); data for 15 (long dotted line), 60 (dotted line) and 200 (short dotted line) GeV/nucleon  $^{16}\text{O}$  are added sequentially.

TABLE I. Statistics  $N_{n\alpha}(^{8}\text{Be})$  among  $n_\alpha$  events of  $^{16}\text{O}$  dissociation; percentage of  $N_{n\alpha}(^{8}\text{Be})$  among  $N_{n\alpha}$  is indicated.

$n_\alpha$	3.65 GeV/nucleon	15 GeV/nucleon	60 GeV/nucleon	200 GeV/nucleon	All
	$N_{n\alpha}(^{8}\text{Be})/N_{n\alpha}(\%)$	$N_{n\alpha}(^{8}\text{Be})/N_{n\alpha}(\%)$	$N_{n\alpha}(^{8}\text{Be})/N_{n\alpha}(\%)$	$N_{n\alpha}(^{8}\text{Be})/N_{n\alpha}(\%)$	$N_{n\alpha}(^{8}\text{Be})/N_{n\alpha}(\%)$
2	32/390 (8 ± 2)	6/95 (6 ± 3)	9/97 (9 ± 3)	3/56 (5 ± 3)	50/638 (8 ± 1)
3	40/176 (23 ± 4)	13/51 (26 ± 8)	12/64 (19 ± 6)	8/29 (28 ± 11)	73/320 (23 ± 3)
4	13/28 (46 ± 15)	1/4 (25)	2/2 (100)	0/1 (0)	16/35 (46 ± 14)

gives grounds to summarize the statistics, confirming the contribution of  $^{8}\text{Be}$ , which grows with  $n_\alpha$  (right column of Table I). 13  $4\alpha$ -events are “white” stars, and 6 of them contain  $^{8}\text{Be}$  decays. This number makes it possible to relate the “white”  $4\alpha$ -star statistics mentioned above with the other  $^{16}\text{O}$  dissociation channels.

Only the  $N_{n\alpha}(^{8}\text{Be})$  statistics at 3.65 GeV/nucleon correspond to the level expected for the  $^{9}\text{B}$  and HS decays. The number of  $2\alpha p$  triplets  $N_{2\alpha p}(^{8}\text{Be})$  under the condition  $Q_{2\alpha}(^{8}\text{Be}) \leq 0.2$  MeV noticeably increases at the origin at  $Q_{2\alpha p}(^{9}\text{B}) \leq 0.5$  MeV (Fig. 2). This criterion

TABLE II. Statistics of  $N_{n\alpha mp}(^9\text{B})$  and  $N_{n\alpha mp}(^8\text{Be})$  decays in the fragmentation channels  $N_{n\alpha mp}(^8\text{Be})$  of  $^{16}\text{O}$  and  $^{22}\text{Ne}$  nuclei with a multiplicity of  $\alpha$ -particles  $n_\alpha$  and protons  $m_p$ .

$N_{n\alpha mp} \ ^{16}\text{O}$	$N_{n\alpha mp}(^9\text{B})/N_{n\alpha mp}(^8\text{Be}) \ (\%)$	$N_{n\alpha mp} \ ^{22}\text{Ne}$	$N_{n\alpha mp}(^9\text{B})/N_{n\alpha mp}(^8\text{Be}) \ (\%)$
338 2 $\alpha$ + (1-4) $p$	9/26 (35 $\pm$ 14)	429 2 $\alpha$ + (1-6) $p$	8/25 (32 $\pm$ 13)
131 3 $\alpha$ + (1,2) $p$	12/31 (39 $\pm$ 13)	203 3 $\alpha$ + (1-4) $p$	8/39 (21 $\pm$ 8)
-	-	58 4 $\alpha$ + (1,2) $p$	4/20 (20 $\pm$ 12)

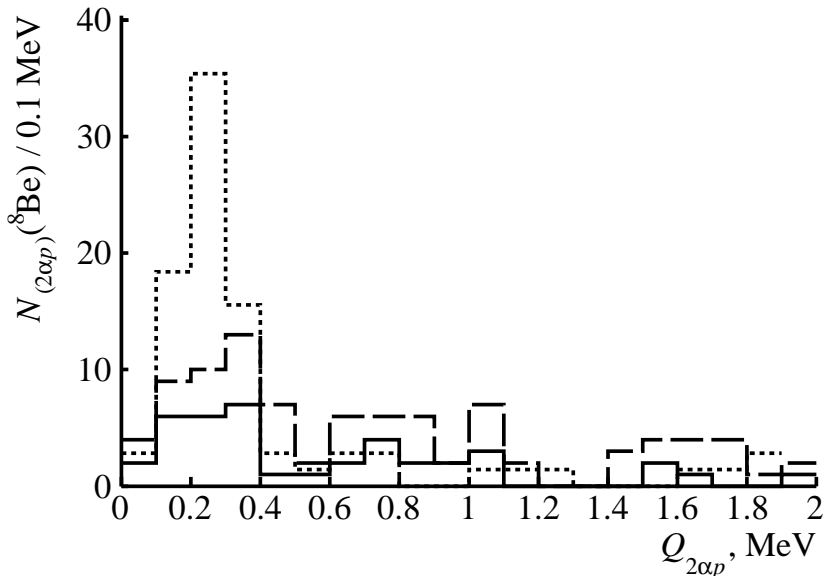


FIG. 2. Distribution of  $2\alpha p$  triplets  $N_{(2\alpha p)}(^8\text{Be})$  over invariant mass  $Q_{2\alpha p} \leq 2$  MeV in 3.65 GeV/nucleon  $^{16}\text{O}$  (solid) and 3.22 GeV/nucleon  $^{22}\text{Ne}$  fragmentation (added by dashed line). Dots mark  $N_{(2\alpha p)}(^8\text{Be})$  distribution in coherent dissociation  $^{10}\text{C} \rightarrow 2\alpha 2p$  (normalized to  $^{16}\text{O}$  and  $^{22}\text{Ne}$  statistics).

is adopted for the  $^9\text{B}$  decays  $N_{2\alpha p}(^9\text{B})$ . It coincides with the precipitation of 54  $^9\text{B}$  decays in the most convenient of coherent dissociation  $^{10}\text{C} \rightarrow 2\alpha 2p$  at 1.2 GeV/nucleon (Fig. 2) [8].

In the channels  $n_\alpha$  with a multiplicity of protons  $m_p$ , on going from  $n_\alpha = 2$  to 3, the number  $N_{n\alpha mp}(^9\text{B})$  increases relative to  $N_{n\alpha mp}(^9\text{B})$  proportionally to  $N_{n\alpha mp}(^8\text{Be})$  (Table II). At  $n_\alpha = 3$ , one HS decay is identified and 5 at  $n_\alpha = 4$ . In the latter case,  $N_{4\alpha}(\text{HS})/N_{n\alpha}(^8\text{Be}) = 0.4 \pm 0.2$  does not contradict the result for “white”  $4\alpha$  stars.

### III. FRAGMENTATION OF $^{16}\text{O}$ ON PROTONS

The accepted approximations can be verified using the data obtained in exposure to 2.4 GeV/nucleon  $^{16}\text{O}$  nuclei of the JINR 1-meter hydrogen bubble chamber (VPK-100), placed in a magnetic field [21]. The dataset includes full solid angle measurements of the momentum vectors of the  $^{16}\text{O} + p$  reaction products in 11104 collisions of all kinds. In this case, there is also a peak in the initial part of the angle distribution of  $2\alpha$ -pairs  $\Theta_{2\alpha}$ , corresponding to  $^8\text{Be}$  decays [21]. As noted [8], when momenta of relativistic He fragments reconstructed with insufficient accuracy are used in the  $Q_{2\alpha}$  calculation, the  $^8\text{Be}$  signal practically disappears. There remains the possibility of moment fixing as in the NTE case, and using the measured values when normalized to the value of the initial momentum per nucleon for the identification of He and H isotopes.

In Fig. 3, the invariant mass distributions of all  $2\alpha$ -pairs  $Q_{2\alpha}$ ,  $2\alpha p$ -triplets  $Q_{2\alpha p}$ , and  $3\alpha$ -triplets  $Q_{3\alpha}$  calculated from the angles determined in the VPK-100, are superimposed. In the presented range, the  $Q_{2\alpha}$  distribution is normalized to the  $Q_{2\alpha p}$  statistics with a decreasing factor of 25. Directly depending on  $\Theta_{2\alpha}$ , the  $Q_{2\alpha}$  variant with fixed momenta demonstrates the  $^8\text{Be}$  peak. According to the measured momenta of fragments, the condition  $Q_{2\alpha}(^8\text{Be}) \leq 0.2$  MeV removes the  $^3\text{He}$  contribution, and the contribution of protons is 90% among H.

The peak in the  $Q_{2\alpha p}$  distribution shown in Fig. 3 with the condition  $Q_{2\alpha}(^8\text{Be}) \leq 0.2$  MeV and selection of protons, indicates 60  $^9\text{B}$  decays to  $Q_{2\alpha p}(^9\text{B}) \leq 0.5$  MeV. The average value  $\langle Q_{2\alpha p} \rangle$  (RMS) =  $271 \pm 15$  (120) keV corresponds to the NTE result [6]. Similarly, the peak in the distribution  $Q_{3\alpha}(\text{HS}) \leq 0.7$  MeV with the condition  $Q_{2\alpha}(^8\text{Be}) \leq 0.2$  MeV corresponds to the identification of 47 HS decays, having  $\langle Q_{3\alpha} \rangle$  (RMS) =  $322 \pm 25$  (180) keV [9]. In the statistics, there are four events with a  $^{28}\text{Be}$  formation and one with coincident candidates  $^9\text{B}$  and HS.

Table III shows the data reflecting the change in contributions from unstable state decays in events with the  $\alpha$ -particles multiplicity  $n_\alpha$  (in this case, identified  $^4\text{He}$  nuclei). With increasing  $n_\alpha$ , the  $^8\text{Be}$  detecting probability increases rapidly. An increase in  $n_\alpha$  leads to a relative decrease in  $N_{n\alpha}(^9\text{B})$ , which can be explained by a decrease in the number of protons available for the  $^9\text{B}$  formation. On the contrary,  $N_{n\alpha}(\text{HS})$  increases due to an increase in the number of  $\alpha$ -particles available for the HS formation. In the coherent dissociation  $^{16}\text{O} \rightarrow$

TABLE III. Statistics of events containing at least one  ${}^8\text{Be}$  decay candidate  $N_{n\alpha}$  ( ${}^8\text{Be}$ ),  ${}^9\text{B}$ , or HS under the condition  $Q_{2\alpha}({}^8\text{Be}) \leq 0.2$  MeV among the  $N_{n\alpha}$  events of fragmentation of  ${}^{16}\text{O}$  nuclei on protons with multiplicity  $n_\alpha$ .

$n_\alpha$	$N_{n\alpha}({}^8\text{Be})/N_{n\alpha}$	$N_{n\alpha}({}^9\text{B})$	$N_{n\alpha}(\text{HS})$
	(% $N_{n\alpha}$ )	(% $N_{n\alpha}({}^8\text{Be})$ )	(% $N_{n\alpha}({}^8\text{Be})$ )
2	111/981 (11 $\pm$ 1)	29 (26 $\pm$ 6)	-
3	203/522 (39 $\pm$ 3)	31 (15 $\pm$ 3)	36 (18 $\pm$ 3)
4	27/56 (48 $\pm$ 11)	-	11 (41 $\pm$ 15)

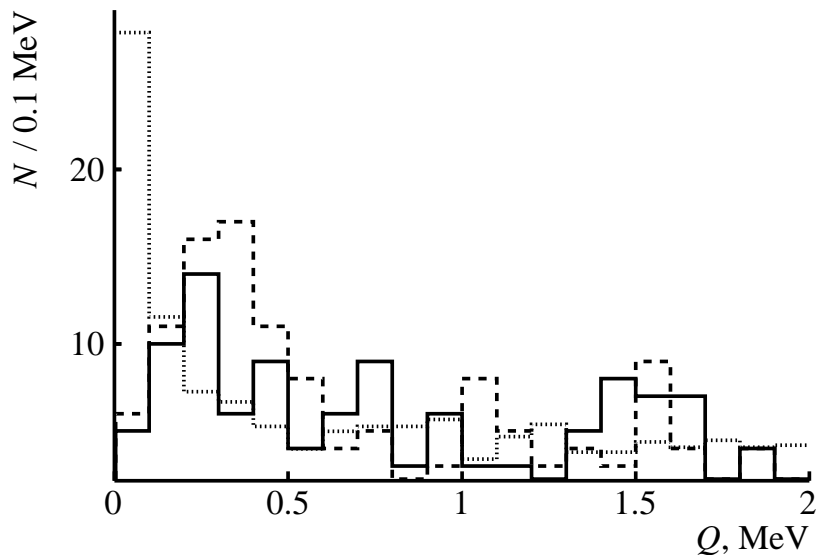


FIG. 3. Distribution of 2.4 GeV/nucleon  ${}^{16}\text{O}$  fragmentation events on protons over invariant masses of all  $2\alpha$ -pairs  $Q_{2\alpha}$  (dots),  $2\alpha p$ -triplets  $Q_{2\alpha p}$  (dashed line) and  $3\alpha$ -triplets  $Q_{3\alpha}$  (solid).

$4\alpha$ , the fraction of HS decays relative to  ${}^8\text{Be}$  is  $35 \pm 1\%$ , which does not contradict to the value for  $n_\alpha = 4$  in the generally more severe  ${}^{16}\text{O} + p$  interaction (Table III). These facts indicate the universality of the appearance of  ${}^8\text{Be}$  and HS.

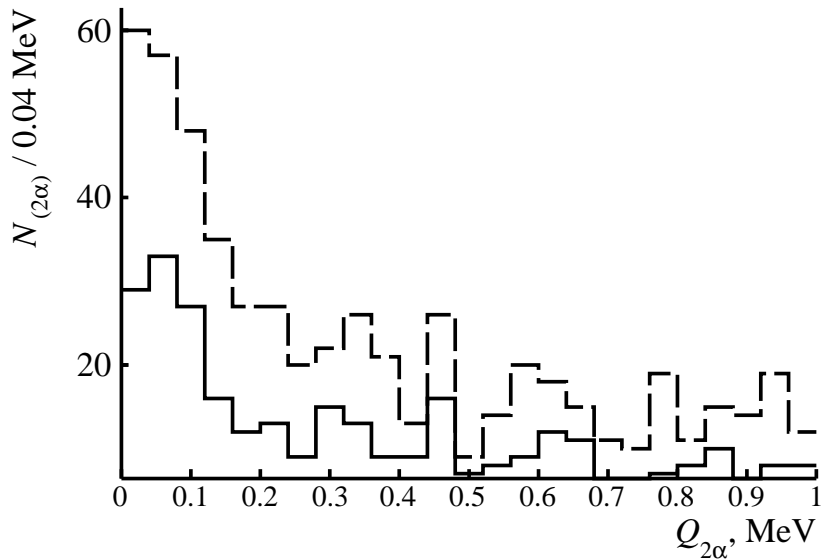


FIG. 4. Distribution of  $2\alpha$ -pairs  $N(2\alpha)$  over invariant mass  $Q_{2\alpha}$  ( $\leq 1$  MeV) in fragmentation of 3.22 GeV/nucleon  $^{22}\text{Ne}$  (solid line) and 14.6 GeV/nucleon  $^{28}\text{Si}$  nuclei (added by dotted line).

#### IV. $^{22}\text{NE}$ AND $^{28}\text{SI}$ FRAGMENTATION

Measurements carried out in NTE layers exposed to  $^{22}\text{Ne}$  nuclei at 3.22 GeV/nucleon (4308 events, JINR Synchrophasotron) and  $^{28}\text{Si}$  at 14.6 GeV/nucleon (1093 events, BNL AGS) further expand the  $n_\alpha$  range. In both cases, no change in the condition  $Q_{2\alpha}(^8\text{Be}) \leq 0.2$  MeV is required (Fig. 4). The  $N_{n\alpha}$  and  $N_{n\alpha}(^8\text{Be})$  statistics are presented in Table. IV. Recently, the  $^{28}\text{Si}$  statistics  $n_\alpha \geq 3$  was tripled by transverse scanning (Table IV). In these cases, the  $^8\text{Be}$  contribution also increases with the  $n_\alpha$  multiplicity.

$^8\text{Be}$  nuclei can arise both directly in fragmentation and via  $^9\text{B}$  and HS decays. Only the  $^{22}\text{Ne}$  statistics makes it possible to estimate the contributions of  $^9\text{B}$  and HS based on the invariant masses  $Q_{2\alpha p}$  and  $Q_{3\alpha}$ . The distribution  $N_{(2\alpha p)}(^8\text{Be})$ , added in Fig. 2 for the  $^{22}\text{Ne}$  case, contains  $2\alpha p$  triplets  $Q_{2\alpha p}(^9\text{B}) \leq 0.5$  MeV. The  $N_{(3\alpha)}(^8\text{Be})$  distribution shown in Fig. 5, contains  $3\alpha$  triplets  $Q_{3\alpha}(\text{HS}) \leq 0.7$  MeV. Previously, this condition was used to establish 41 candidates for HS decays in the dissociation  $^{12}\text{C} \rightarrow 3\alpha$  from the  $N_{(3\alpha)}(^8\text{Be})$  distribution in Fig. 4. Similarly to the case of  $^{16}\text{O}$ , on going from  $n_\alpha = 2$  to 4 for  $^9\text{B}$ ,  $N_{n\alpha mp}(^9\text{B})$  relative to  $N_{n\alpha mp}$  increases (Table II). Transition from  $n_\alpha = 3$  to 4 indicates a noticeable increase in

TABLE IV. Statistics of events  $N_{n\alpha}(^8\text{Be})$  among  $N_{n\alpha}$  events in dissociation of  $^{22}\text{Ne}$  and  $^{28}\text{Si}$  nuclei; the percentage of  $N_{n\alpha}(^8\text{Be})$  among  $N_{n\alpha}$  is indicated.

$n_\alpha$	$^{22}\text{Ne}$ 3.22 GeV/nucleon	$^{28}\text{Si}$ 15 GeV/nucleon	$^{28}\text{Si}$ 15 GeV/nucleon
	$N_{n\alpha}(^8\text{Be})/N_{n\alpha}$ (%)	$N_{n\alpha}(^8\text{Be})/N_{n\alpha}$ (%)	$N_{n\alpha}(^8\text{Be})/N_{n\alpha}$ (%)
2	30/528 (6 $\pm$ 1)	5/164 (3 $\pm$ 2)	$n_\alpha \geq 3$
3	45/243 (19 $\pm$ 3)	10/75 (13 $\pm$ 5)	33/231 (14 $\pm$ 3)
4	25/80 (31 $\pm$ 6)	11/25 (44 $\pm$ 16)	39/121 (32 $\pm$ 6)
5	6/10 (60 $\pm$ 31)	8/17 (47 $\pm$ 20)	16/42 (38 $\pm$ 11)
6	-	1/1 (100)	4/6 (67 $\pm$ 43)

TABLE V. Statistics of events  $N_{n\alpha}(\text{HS})$  among events  $N_{n\alpha}$  in dissociation of  $^{22}\text{Ne}$  nuclei; the percentage of  $N_{n\alpha}(^8\text{Be})$  among  $N_{n\alpha}$  is indicated.

$n_\alpha$	$N_{n\alpha}(\text{HS})/N_{n\alpha}$ (% $N_{n\alpha}$ )	$N(\text{HS})/N_{n\alpha}(^8\text{Be})$ , %
3	3/243 (1.2 $\pm$ 0.6)	7 $\pm$ 4
4	10/80 (13 $\pm$ 5)	40 $\pm$ 15
5	1/10	17

HS, showing an analogy with the  $^{16}\text{O}$  data as well (Table V).

## V. $^{197}\text{AU}$ FRAGMENTATION

There are similar measurements of 1316 interactions of  $^{197}\text{Au}$  nuclei at 10.7 GeV/nucleon (BNL AGS, 90s). For this dataset, Fig. 6a shows the distribution of  $2\alpha$ -pairs at small values of  $Q_{2\alpha}$ . Due to the deteriorated resolution, the  $^8\text{Be}$  region expands, which requires softening the selection of  $Q_{2\alpha}(^8\text{Be}) \leq 0.4$  MeV to maintain efficiency. Further, to check the  $N_{n\alpha}(^8\text{Be})$  correlation and minimize the background in  $N_{n\alpha}(^9\text{B})$  and  $N_{n\alpha}(\text{HS})$ , the condition  $Q_{2\alpha}(^8\text{Be}) \leq 0.2$  MeV is also applied. The distributions of  $2\alpha p$ -triplets,  $3\alpha$ -triplets, and  $4\alpha$ -quartets in the small  $Q$  regions of events in which, according to these conditions, there is at least one candidate for  $^8\text{Be}$  decay are also included in Fig. 6. Note that the distributions (b) and (c) contain  $2\alpha p$  and  $3\alpha$  triplets satisfying the conditions  $Q_{2\alpha p}(^9\text{B}) \leq 0.5$  MeV and  $Q_{3\alpha}(\text{HS}) \leq$

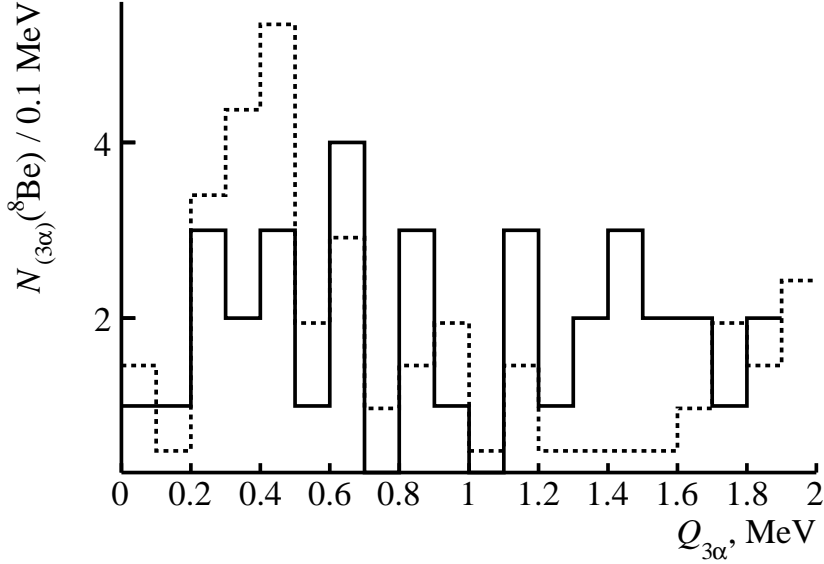


FIG. 5. Distribution of  $3\alpha$ -triplets  $N_{(3\alpha)}(^8\text{Be})$  over invariant mass  $Q_{2\alpha p}$  ( $\leq 2$  MeV) in 3.22 GeV/nucleon  $^{22}\text{Ne}$  fragmentation (solid line). Dots mark distribution  $N_{(3\alpha)}(^8\text{Be})$  in dissociation  $^{12}\text{C} \rightarrow 3\alpha$  normalized to  $^{22}\text{Ne}$  statistics.

0.7 MeV, respectively.

Statistics and relative yields of the unstable states are presented in Table. VI with allowance for  $Q_{2\alpha}(^8\text{Be}) \leq 0.4$  MeV. Channels  $n_\alpha \geq 11$  are summed to reduce errors. The ratio of the number of events  $N_{n\alpha}(^8\text{Be})$  including at least one  $^8\text{Be}$  decay candidate to the statistics of the channel  $N_{n\alpha}$ , grows rapidly to  $n_\alpha = 10$  to about 0.5. This trend persists when the condition is tightened to  $Q_{2\alpha}(^8\text{Be})$  despite the decrease in statistics (Fig. 7).

The ratio of the number of events  $N_{n\alpha}(^9\text{B})$  and  $N_{n\alpha}(\text{HS})$  to the statistics  $N_{n\alpha}(^8\text{Be})$  shows no noticeable change with multiplicity  $n_\alpha$  (Table VI). The statistics of the identified decays of  $^8\text{Be}$  pairs  $N_{n\alpha}(^8\text{Be})$  behave in the same way. In fact, these three ratios indicate an increase in  $N_{n\alpha}(^9\text{B})$ ,  $N_{n\alpha}(\text{HS})$  and  $N_{n\alpha}(^8\text{Be})$  relative to  $N_{n\alpha}$ . In these three cases, significant statistical errors make it possible to characterize only general trends. Summing the statistics on the multiplicity  $n_\alpha$  and normalizing to the sum  $N_{n\alpha}(^8\text{Be})$  leads to the relative contributions  $N_{n\alpha}(^9\text{B})$ ,  $N_{n\alpha}(\text{HS})$ , and  $N_{n\alpha}(^8\text{Be})$  equal to  $25 \pm 4\%$ ,  $6 \pm 2\%$ , and  $10 \pm 2\%$ , respectively.

The distribution over  $Q_{4\alpha}$  (Fig.6d) indicates near-threshold  $4\alpha$ -quadruples, in which the decays of HS and  $^{28}\text{Be}$  are reconstructed with the condition  $Q_{2\alpha}(^8\text{Be}) \leq 0.2$  MeV, including  $Q_{4\alpha} = 1.0$  ( $16\alpha$ , HS), 1.9 ( $11\alpha$ , HS), 2.1 ( $9\alpha$ ,  $^{28}\text{Be}$ ), 2.2 ( $5\alpha$ ,  $^{28}\text{Be}$ ), 2.4 ( $9\alpha$ , HS) MeV. The

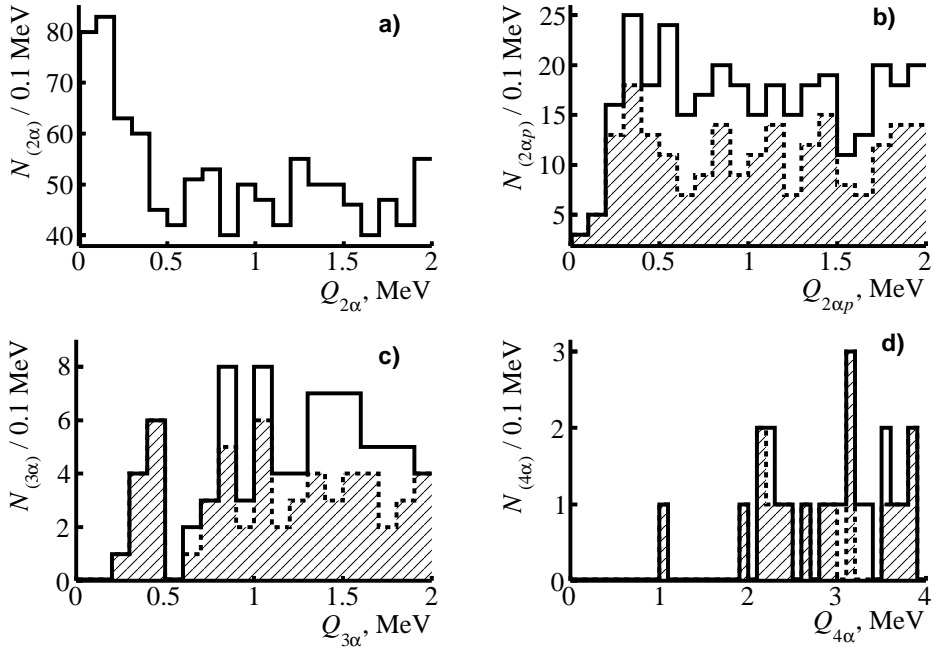


FIG. 6. Distributions over invariant masses  $Q$  of  $2\alpha$ -pairs (a) in fragmentation of  $^{197}\text{Au}$  nuclei, as well as  $2\alpha p$ -triplets (b),  $3\alpha$ -triplets (c), and  $4\alpha$ -quartets (d) in events with  $^8\text{Be}$  candidate selected according to  $Q_{2\alpha}(^8\text{Be}) \leq 0.4$  MeV (solid) and  $\leq 0.2$  MeV (shaded).

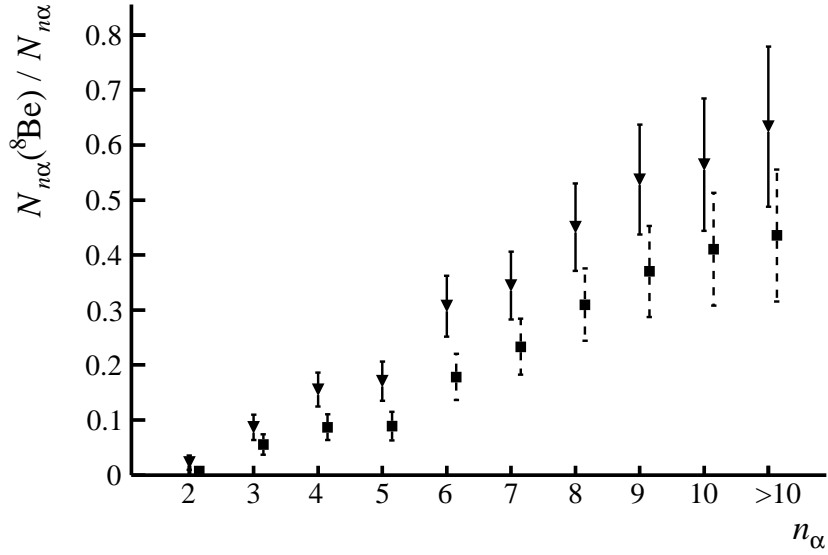


FIG. 7. Dependence of relative contribution of  $N_{n\alpha}(^8\text{Be})$  decays to the statistics  $N_{n\alpha}$  of events with  $\alpha$ -particle multiplicity  $n_\alpha$  in fragmentation of  $^{197}\text{Au}$  nuclei upon selection  $Q_{2\alpha}(^8\text{Be}) \leq 0.4$  MeV (triangles) and  $\leq 0.2$  MeV (squares).

TABLE VI. Statistics of events containing at least one  ${}^8\text{Be}$ ,  ${}^9\text{B}$  or HS decay, or at least two  ${}^8\text{Be}$  provided  $Q_{2\alpha}({}^8\text{Be}) \leq 0.4$  MeV among the events  $N_{n\alpha}$  of  ${}^{197}\text{Au}$  fragmentation with multiplicity  $n_\alpha$ ; the total statistics of the channels  $n_\alpha \geq 11$  are highlighted.

$n_\alpha$	$N_{n\alpha}({}^8\text{Be})/N_{n\alpha}$ (% $N_{n\alpha}$ )	$N_{n\alpha}({}^9\text{B})$ (% $N_{n\alpha}({}^8\text{Be})$ )	$N_{n\alpha}(\text{HS})$ (% $N_{n\alpha}({}^8\text{Be})$ )	$N_{n\alpha}(2{}^8\text{Be})$ (% $N_{n\alpha}({}^8\text{Be})$ )
2	3/133 (2 $\pm$ 1)	-	-	-
3	14/162 (9 $\pm$ 3)	1 (7)	-	-
4	25/161 (16 $\pm$ 4)	7 (28 $\pm$ 12)	2 (8 $\pm$ 6)	-
5	23/135 (17 $\pm$ 4)	5 (22 $\pm$ 11)	-	1 (4)
6	31/101 (31 $\pm$ 7)	9 (29 $\pm$ 11)	2 (6 $\pm$ 4)	-
7	31/90 (34 $\pm$ 7)	6 (19 $\pm$ 9)	2 (6 $\pm$ 4)	3 (10 $\pm$ 6)
8	32/71 (45 $\pm$ 10)	8 (25 $\pm$ 10)	2 (6 $\pm$ 4)	2 (7 $\pm$ 5)
9	29/54 (54 $\pm$ 13)	9 (31 $\pm$ 12)	3 (10 $\pm$ 6)	5 (17 $\pm$ 8)
10	22/39 (56 $\pm$ 15)	4 (18 $\pm$ 10)	-	5 (23 $\pm$ 12)
11	10/15 (67 $\pm$ 27)	3 (30 $\pm$ 20)	1 (10)	2 (20 $\pm$ 16)
	19/30 (63 $\pm$ 19)	7 (37 $\pm$ 16)	2 (11 $\pm$ 8)	6 (32 $\pm$ 15)
12	2/5	1	-	1
13	2/4	1	-	1
14	3/3	1	-	1
15	1/1	-	-	-
16	1/2	1	1	1

$0_6^+$  excitation of the  ${}^{16}\text{O}$  nucleus at 660 keV above the  $4\alpha$ -threshold is assumed to be a  $4\alpha$ -condensate [12, 13]. It could decay in the sequence the decay of which could proceed along the chain  ${}^{16}\text{O}(0_6^+) \rightarrow {}^{12}\text{C}(0_2^+) \rightarrow {}^8\text{Be}(0^+) \rightarrow 2\alpha$  or  ${}^{16}\text{O}(0_6^+) \rightarrow 2{}^8\text{Be}(0^+) \rightarrow 4\alpha$ . Investigation of this problem requires a qualitatively different level of  $n_\alpha$ -ensemble statistics, which, in principle, is available in the transverse event search.

## VI. SUMMARY

The preserved and recently supplemented data on the relativistic fragmentation of  $^{16}\text{O}$ ,  $^{22}\text{Ne}$ ,  $^{28}\text{Si}$ , and  $^{197}\text{Au}$  nuclei in a nuclear track emulsion made it possible to identify decays of  $^8\text{Be}$ ,  $^9\text{B}$  nuclei and Hoyle state in the invariant mass distributions of  $2\alpha$ -pairs,  $2\alpha p$ - and  $3\alpha$ -triplets. The determination of the invariant mass from the angles of emission of fragments in the velocity conservation approximation turns out to be an adequate approximation. Starting with the  $^{16}\text{O}$  fragmentation, the presented analysis indicates a relative enhancement in the  $^8\text{Be}$  contribution with an increase in the number of relativistic  $\alpha$ -particles per event and the remaining proportional contributions of HS and  $^9\text{B}$ . In the  $^{197}\text{Au}$  fragmentation, the tendency is traced up to at least 10 relativistic  $\alpha$ -particles per event. This observation makes it possible to propose a development of the theory of relativistic fragmentation of nuclei taking into account the interactions of  $\alpha$ -particles, which are characteristic of low-energy nuclear physics.

It is obvious that it is necessary to increase the statistics of events with a high multiplicity of  $\alpha$ -particles with special attention to the accuracy of measurements of the emission angles of relativistic He and H fragments. An analysis of the data on the  $^{16}\text{O}$  fragmentation in the hydrogen bubble chamber confirms the approximations and conclusions made. The application of this method would be productive for light isotopes, including radioactive ones. Unfortunately, it has gone down in history, and its renewal does not seem real. The feasibility of this approach by other methods of high energy physics has not yet been demonstrated. Therefore, the use of the flexible method of nuclear track emulsion retains a prospect for the study of unstable states produced in a narrow cone of relativistic fragmentation by nuclei in the widest range of mass numbers.

New possibilities are contained in existing layers exposed to 800-950  $A$  MeV  $^{84}\text{Kr}$  nuclei (SIS synchrotron, GSI, early 90s) that were already used for the reaction multiplicity survey [22]. To limit the uncertainty associated with the deceleration of the beam nuclei, the analysis was performed on a small NTE section. In principle, the decrease in energy can be calculated and taken into account in the calculation of the invariant masses. Thus, the covered energy range and the viewed NTE area can be radically extended. This development is in the near future. Note that the reconstruction of  $^8\text{Be}$  and the Hoyle state in the presented

approach was successfully performed in the 400 MeV/nucleon  $^{12}\text{C}$  case [6].

---

- [1] P.I. Zarubin, Lect. Notes in Phys., 875, Clusters in Nuclei, Volume 3. Springer Int. Publ., 51 (2013); DOI: 10.1007/978-3-319-00875-0\_1
- [2] D.A. Artemenkov, A. A. Zaitsev, P. I. Zarubin, Phys. Part. Nucl. 48 147(2017); DOI: 10.1134/S1063779617060047
- [3] D.A. Artemenkov *et al.*, Phys. At. Nucl. 80, 1126 (2017); DOI:10.1134/S1063778817060047.
- [4] V.V. Belaga, A.A. Benjaza, V.V. Rusakova, D.A. Salomov, G.M. Chernov, Phys. At. Nucl. 58, 1905 (1995); DOI: 10.1007/BF01010000
- [5] N.P. Andreeva *et al.*, Phys. At. Nucl. 59, 102 (1996); arXiv:1109.3007.
- [6] D.A. Artemenkov *et al.*, Rad. Meas. 119, 199 (2018); DOI: 10.1016/j.radmeas.2018.11.005.
- [7] D.A. Artemenkov *et al.*, Springer Proc. Phys. 238, 137 (2020); DOI: 10.1007/978-3-030-32357-8\_24.
- [8] D.A. Artemenkov *et al.*, Eur. Phys. J. A 56, 250 (2020); DOI: 10.1140/epja/s10050-020-00252-3
- [9] B. Borderie *et al.*, Phys. Lett. B 755, 475 (2016) ; DOI: 10.1016/j.physletb.2016.02.061.
- [10] K. Schmidt *et al.*, Phys. Rev. C 95, 054618 (2017); DOI: 10.1103/PhysRevC.95.054618.
- [11] M. Barbui *et al.*, Phys. Rev. C 98, 044601 (2018); DOI: 10.1103/PhysRevC.98.044601.
- [12] A. Tohsaki, H. Horiuchi, P. Schuck and G. Röpke, Rev. Mod. Phys. 89, 011002 (2017); DOI: 10.1103/RevModPhys.89.011002
- [13] T. Yamada and P. Schuck, Phys. Rev. C 69, 024309 (2004); DOI: 10.1103/PhysRevC.69.024309.
- [14] LM. Satarov, R.V. Poberezhnyuk, I. N. Mishustin, and H. Stoecker Phys. Rev. C 103, 024301 (2021); DOI: 10.1103/PhysRevC.103.024301
- [15] N.P. Andreeva *et al.*, Sov. J. Nucl. Phys. 47 102 (1988); Yad. Fiz. 47 157 (1988) and Dubna JINR - 86-828.
- [16] A. El-Naghy *et al.*, J. Phys. G, 14 1125 (1988); DOI: 10.1088/0305-4616/14/8/015
- [17] M.I. Adamovich *et al.*, Phys. Rev. C 40, 66 (1989); DOI: 10.1103/PhysRevC.40.66
- [18] M.I. Adamovich *et al.*, Z. Phys. A 351, 311 (1995); DOI: 10.1007/BF01290914.
- [19] M.I. Adamovich *et al.*, Eur. Phys. J. A 5, 429 (1999); DOI: 10.1007/s100500050306.
- [20] The BECQUEREL Project <http://becquerel.jinr.ru/movies/movies.html>.
- [21] V.V. Glagolev *et al.*, Eur. Phys. J. A 11, 285 (2001); DOI: 10.1007/s100500170067.
- [22] S.A. Krasnov *et al.*, Czechoslovak J. of Phys. 46 531 (1996); DOI: 10.1007/BF01690674